Regulation of Cilia Abundance in Multiciliated Cells

Rashmi Nanjundappa[1], Dong Kong[2], Kyuhwan Shim[1], Tim Stearns[3], Steven L. Brody[4], Jadranka Loncarek[2], and Moe R. Mahjoub[1,5] *.

1 - Department of Medicine (Nephrology Division), Washington University, St Louis, MO
2 - Center for Cancer Research, National Cancer Institute, Frederick, MD
3 - Department of Biology, Stanford University, Stanford, CA
4 - Department of Medicine (Pulmonary Division), Washington University, St Louis, MO
5 - Department of Cell Biology and Physiology, Washington University, St Louis, MO

*** Corresponding author:**

Moe R. Mahjoub, Ph.D.
Department of Medicine
Washington University School of Medicine
Campus Box 8126
660 South Euclid Avenue
St Louis, MO 63110
Email: mmahjoub@wustl.edu
Phone: (314) 362-5681
FAX: (314) 362-8237

Keywords: centriole, basal body, cilia, multiciliated, deuterosome, airway.

Abstract:

Multiciliated cells (MCC) are specialized epithelia that contain hundreds of motile cilia used to propel fluid over the surface of the cell. To template these cilia, each MCC produces hundreds of centrioles by a process termed centriole amplification. Airway progenitor cells initially contain two parental centrioles that nucleate multiple centrioles at once, and structures called deuterosomes that assemble the vast majority of centrioles during amplification. Remarkably, how each cell regulates the precise number of its centrioles and cilia remains unknown. Here, we investigate mechanisms that establish centriole number in MCC using an *ex vivo* airway culture model. We show that ablation of parental centrioles, via inhibition of Plk4 kinase, does not perturb deuterosome formation and centriole amplification, nor alter the total complement of centrioles per cell. Airway MCC vary in size and surface area, and exhibit a broad range in centriole number. Quantification of centriole abundance *in vitro* and *in vivo* identified a direct relationship between cell-surface area and centriole number. By manipulating cell size and shape, we discovered that centriole number scales with increasing surface area. Collectively, our results demonstrate that parental centrioles and Plk4 are dispensable for deuterosome formation, centriole amplification, and establishment of centriole number. Instead, a cell-intrinsic surface area-dependent mechanism controls centriole and cilia abundance in multiciliated cells.

Introduction:

In mammals, multiciliated cells (MCC) are terminally differentiated epithelia that line the respiratory tract, brain ventricles and segments of the female and male reproductive organs [1, 2]. Each MCC contains hundreds of motile cilia, microtubule-based organelles that generate the motive force to move fluid over the surface of the cell. In the airway, motile cilia of MCC beat directionally to propel mucus and inhaled contaminants out of the lungs. Ciliary motility of ependymal MCC lining the brain ventricles is key for movement of cerebrospinal fluid through the central nervous system, while cilia on MCC in the reproductive tracts are important for ovum and sperm transport [1, 2]. Thus, the proper assembly of hundreds of motile cilia is critical for the functions of MCC, and the overall health of the associated tissues. Mutations that result in reduced cilia abundance cause human diseases due to aberrant cilia-based fluid flow [3-6], suggesting that establishment of the correct number of cilia per cell is important for function. MCC in different tissues display significant variability in motile cilia number, ranging from 30-600 cilia per cell [1, 2]. However, a major unresolved question is how each cell regulates the precise number of its motile cilia during differentiation.

To template these cilia, each MCC undergoes a process termed centriole amplification to produce hundreds of centrioles, barrel-shaped microtubule structures that form the base upon which cilia are assembled. In the airway, proliferating progenitors (called basal cells) initially contain a single centrosome with two parental centrioles (PC), which they maintain via the canonical centriole duplication mechanism (Fig. 1a, [7-9]). During MCC differentiation, the post-mitotic basal cells undergo massive centriole production that was thought to occur through two parallel pathways: a parental centriole-dependent pathway whereby the original PC template the assembly of multiple procentrioles simultaneously, and an acentriolar or "*de novo"* pathway mediated by dozens of deuterosomes, spheroidal electron-dense structures that are capable of producing multiple procentrioles (Fig. 1a, [8, 10, 11]). Deuterosomes are transient structures that are absent in proliferating progenitor cells, are formed during early centriole amplification, and mostly disappear after centriologenesis is complete [12, 13]. Although both PC-dependent and deuterosome-dependent pathways have been known for decades, the molecular mechanisms that govern the two pathways and their relative contributions to the total complement of centrioles has remained enigmatic.

Most of the key proteins involved in canonical centriole duplication play an essential role in both PC- and deuterosome-dependent centriole amplification pathways in MCC [9, 12-15]. This

indicates that centriole duplication in cycling cells and centriole amplification in MCC share common and conserved molecular mechanisms despite their morphological differences. However, recent studies have characterized proteins that are uniquely associated with deuterosomes. For example, Deup1 and Ccdc78 were recently identified as deuterosome-specific proteins that are essential for the formation of deuterosomes and, subsequently, centriole amplification [12, 13]. These data support the theory that the PC-dependent and deuterosome-dependent centriole amplification pathways act in parallel, but use unique molecular components to produce all of the centrioles in a cell. It has been estimated that the deuterosome-dependent pathway contributes the majority (80-90%) of the total centrioles assembled during amplification, while the PC-dependent pathway contributes roughly 10-20% towards the final number [2, 8, 13, 16]. Intriguingly, a recent study found that deuterosomes themselves are nucleated from the original PC, indicating that these two pathways may not be independent of each other after all [16]. If true, this would suggest that all centrioles produced in MCC are ultimately dependent on the PC. Yet, a number of important questions have remained unanswered: are parental centrioles necessary for deuterosome biogenesis? What is the actual contribution of the PC to final centriole number? How do cells that start with exactly two parental centrioles generate such a variable number during differentiation?

In this study, we sought to determine the mechanisms by which airway MCC establish centriole number, using an *ex vivo* airway culture system [17-19]. We began by testing the hypothesis that parental centrioles are essential for deuterosome formation. To ablate PC during proliferation, we used a small molecule inhibitor and shRNA-mediated depletion of Plk4, the major kinase involved in centriole duplication [7, 20]. Surprisingly, loss of parental centrioles did not affect deuterosome formation, indicating that PC are dispensable for deuterosome biogenesis. Moreover, the loss of PC and Plk4 function did not disrupt centriole amplification nor decrease the total number of centrioles per cell. Thus, establishment of centriole abundance is regulated by a different cellular property. Airway MCC vary in size and surface area, and display a wide range in centriole number. Quantification of centriole abundance *in vitro* and *in vivo* highlighted a direct relationship between cell-surface area and centriole number. To determine if cell size was a major determinant of centriole abundance, we cultured basal cells on an extracellular matrix of increasing density to manipulate size. We found that centriole number scales with increasing surface area, but not volume, of multiciliated cells. Together, our results point to a cell-intrinsic, surface area-dependent mechanism that establishes centriole-cilia abundance in airway multiciliated cells.

Results:

Parental centrioles are dispensable for centriole amplification

We previously established a mouse tracheal epithelial cell (MTEC) culture system to study centriologenesis and ciliary assembly in MCC [14, 18, 19, 21]. This airway model entails seeding freshly isolated mouse tracheal basal cells onto a porous filter suspended in medium, and allowing the progenitors to proliferate into a confluent, polarized layer. Cells are induced to differentiate into MCC and other cell types found in the airway (for example, secretory cells) by exposure to an air–liquid interface (ALI). During proliferation, basal cells contain two centrosomal centrioles that are maintained via the canonical centriole duplication mechanism (Fig. 1a). During post-mitotic MCC differentiation, the centriologenesis program proceeds in distinct stages from ALI days 0 to 12: centriolar protein aggregates and deuterosomes form near the PC, and procentrioles are nucleated from both PC and deuterosomes (stage I, ALI1-2); procentrioles continue to grow and elongate from PC and deuterosomes (stage II, ALI3-4); centrioles disengage from PC and deuterosomes, start to mature into basal bodies and migrate towards the apical membrane (stage III, ALI4-8); fully mature, apically docked basal bodies template ciliary assembly (stage IV, ALI8-12). By ALI12, most cells have completed differentiation into fully mature MCC (Fig. 1a).

It was recently proposed that deuterosomes are nucleated from the original PC, suggesting that the *de novo* centriole assembly pathway is dependent on PC [16]. To test this theory, we ablated PC in basal cells using Centrinone [22], a selective inhibitor of the kinase Plk4 known as the "master regulator" of centriole assembly [20, 23-26]. Centrinone blocks centriole duplication, resulting in cells that lack centrioles following a few rounds of cell division [22]. Basal cells were cultured with or without 1 μM Centrinone, roughly 3-8 times higher concentrations than needed to suppress centriole formation in most cells [22], and the compound was maintained in the medium throughout differentiation (described in Methods). Samples were fixed at various stages of differentiation, immunostained for centrioles and analyzed using either confocal or superresolution structured illumination microscopy (3D-SIM). Control cells at ALI0 predominantly contain the original two PC (Fig.1b-c). Upon exposure to ALI, cells proceeded through the various stages of centriole amplification, resulting in a population of cells comprised of roughly 60% MCC and 40% non-MCC as expected (Fig. 1c). Growth of basal cells in the presence of 1 μM Centrinone resulted in >80% of cells lacking PC at ALI0 (Fig. 1b-c). Remarkably, the formation of centriolar aggregates and subsequent centriole amplification proceeded normally in the absence of PC. Moreover, there was no significant difference in the timing of centriologenesis, or the fraction of MCC in the population

(Fig. 1b-c). To ensure that Centrinone-treated cells were indeed lacking PC prior to differentiation, we analyzed cells using transmission electron microscopy (TEM). Cells at ALI0 were serially sectioned beginning at the apical surface and down to the basal membrane. Whereas PC were evident in control cells, there was >80% decrease in cells containing PC upon Centrinone treatment (Fig. 1d and Supplementary Video 1), consistent with the immunofluorescence analysis.

The abundance of Plk4 protein is regulated by autophosphorylation-induced degradation [27]. Centrinone-mediated inhibition of Plk4 kinase activity blocks this degradation, resulting in elevated (yet inactive) Plk4 protein levels [22]. In control cells, Plk4 expression increased during early stages of centriole amplification, peaking at ALI3 and subsequently decreasing upon centriole maturation at ALI8 (Fig. 2a-b). Centrinone-treated cells showed accumulation of Plk4, which was already evident in a higher proportion of cells at ALI0-1 (Fig. 2a). Unlike control cells, the high Plk4-expressing fraction persisted at ALI8 and beyond (Fig. 2a-b), indicating that Plk4 kinase activity was indeed blocked. Moreover, the non-multiciliated cells in the population did not reform/regain their PC (Fig. 1c), further indicative of Centrinone's inhibitory activity in our assay. Finally, we examined whether loss of PC attenuated the various stages of centriole assembly. Control and Centrinone-treated cells were immunostained for markers of procentriole initiation (Sas6, Cep152, Cep135 [28-31]), centriole growth (Cep120, centrin, γ-tubulin [14, 32-36]), centriole maturation (Cep164 [37]), and ciliogenesis (acetylated-tubulin). Loss of PC did not affect the overall timing of centriole amplification stages, or the fraction of MCC in the population (Fig. 2c-g and Supplementary Fig. 1-2). Centriole maturation and ciliogenesis were also unaffected upon loss of PC and Plk4-inhibition (Supplementary Fig. 3). Collectively, these results indicate that parental centrioles and Plk4 kinase activity are not necessary for centriole amplification and ciliogenesis in airway MCC.

Parental centrioles are dispensable for deuterosome formation and centriole abundance

Next, we tested whether loss of PC altered the expression pattern or number of deuterosomes in MCC. Cells at ALI3 were immunostained for Deup1, a core component of deuterosomes essential for their formation [13]. In control cells, deuterosome formation begins ~ALI1 and peaks at ALI3, and they are subsequently lost by ALI8 (Fig. 3a-b). Surprisingly, Deup1 expression was grossly unchanged in cells lacking PC (Fig. 3a-b). However, Deup1 foci were evident in a higher proportion of cells at ALI1, suggesting that deuterosome formation may start sooner in PC-less cells. Since MCC are variable in size and centriole number (discussed in more detail in the subsequent section), we measured deuterosome number and cell surface area (using ZO-1 to outline apical cell-cell junctions), then compared deuterosome abundance in cells of similar

size (Fig. 3c). Centrinone-treated cells lacking PC displayed a slight but significant increase in average deuterosome number per cell (Fig. 3d). Serial-section TEM analysis of cells at ALI3 confirmed the presence of deuterosome structures that were nucleating procentrioles in PC-less cells (Fig. 3e). These deuterosomes appeared consistent in size and morphology with control cells.

The deuterosome-dependent pathway is thought to contribute the majority (80-90%) of centrioles assembled during amplification, whereas the PC-dependent pathway contributes roughly 10-20% towards the final complement [2, 8, 13, 16]. Therefore, we reasoned that loss of PC might result in a reduction in the final complement of centrioles in mature MCC. Quantification of centriole number in control cells at ALI12 showed a range from 100-500, and correlated with increasing surface area (Fig. 4a-b). Loss of PC in Centrinone-treated cells did not disrupt this relationship (Fig. 4c). Importantly, the average number of centrioles per mature MCC did not decrease; in contrast we noted a slight but significant increase in centriole abundance and density (Fig. 4d-e). All together, these results indicate that loss of PC does not inhibit deuterosome biogenesis nor result in decreased centriole abundance in MCC.

Modulating Plk4 expression delays centriole assembly but does not affect number

We were surprised to discover that inhibiting Plk4 activity had no detrimental effect on centriole amplification, as this kinase is known to play a critical role in centriole assembly in the majority of cell types examined in mammals. Plk4 expression becomes elevated during centriole amplification in airway MCC [38], where it localizes to both PC and deuterosomes [13], thus it has been generally assumed to play an important role in centriole amplification. However, our Centrinone treatments suggest that although Plk4 kinase activity is necessary for centriole duplication during the proliferation phase of basal cells, it is not essential for post-mitotic centriole amplification (Fig. 1-3). One possibility is that Plk4 acts in a kinase-independent manner to control centriole amplification, for example as a scaffold to recruit other components of the centriole assembly pathway. To test this, we depleted the protein in basal cells using shRNA-expressing lentivirus. Depletion of Plk4 during the proliferation phase resulted in near complete loss of PC by ALI0 (Fig. 5a-b), similar to the Centrinone experiments. Examination of cells at ALI3 showed that cells lacking Plk4 still initiate centriologenesis similar to control cells (Fig. 5a, c and d), and form more deuterosomes on average (Fig. 5a and e), consistent with the Centrinone-mediated experiments. Moreover, quantification of the fraction of MCC at ALI12 showed no overall difference between control and Plk4-depleted cells. However, the process of centriole amplification appeared delayed, as roughly 50% of Plk4-depleted

cells at ALI12 were in Stages I-II or III-IV instead of being fully mature MCC (Fig. 5a and f). We interpret these results to suggest that loss of Plk4 delays the process, but does not impact overall centriole assembly. Indeed, culturing these Plk4-depleted cells for an additional 9 days caused an increase in the fraction of mature MCC (Fig. 5a and g). Importantly, once cells completed maturation we did not observe a significant decrease in centriole number per cell (Fig. 5h). These results indicate that loss of Plk4 does not impact centriole abundance, consistent with observations using Centrinone.

Loss of PC and Plk4 function did not affect centriole abundance in mature MCC, suggesting that establishment of centriole number is not dependent on them. To further test this hypothesis, we induced the formation of excess PC in basal cells by overexpressing Plk4, which drives nucleation of ectopic centrioles in a diversity of cells and organisms [20, 26]. To overexpress Plk4 in a temporally controlled manner, we used a recently developed mouse model (*Tg::mChPlk4*) whereby mCherry-tagged Plk4 is regulated by tamoxifen-induced Cre-recombinase expression [39, 40]. To conditionally express Plk4 in MTEC, we bred *Tg::mChPlk4* mice to a *Tg::Rosa26-Cre^{ERT2}* [41] strain that globally expresses Cre upon tamoxifen addition. Basal cells were harvested from trachea of *Tg::mChPlk4/Rosa26-Cre^{ERT2}* mice, and MTEC cultures established in the presence or absence of tamoxifen. Constitutive expression of mChPlk4 during the proliferation stage resulted in cells that contained more than the normal complement of two PC at ALI0 (Fig. 5i). However, mature MCC containing excess PC and Plk4 protein formed a similar number of centrioles when compared to control cells at ALI12 (Fig. 5i-j). In sum, manipulating Plk4 protein levels does not alter deuterosome or basal body number, nor does increasing the complement of parental centrioles.

Centriole number scales with surface area

Since establishment of centriole abundance appears to be independent of the PC-deuterosome mediated pathway, we wondered if other cellular properties influenced centriole-cilia abundance. We discovered that airway multiciliated cells grown *in vitro* display a broad range in centriole number, from 100-500 centrioles per cell (Fig. 4). We wanted to determine whether this broad range in centriole number, and its relationship to surface area, was retained *in vivo*. Trachea isolated from wild-type mice was cut longitudinally to expose the lumen, immunostained with centrin and ZO-1, then imaged by 3D-SIM (Fig. 6a). Quantification of centriole number showed a similar variation in centriole abundance (Fig. 6b). Consistent with the measurements *in vitro*, there was a

direct relationship between centriole number and surface area, as larger MCC contained more centrioles compared with smaller cells (Fig. 6b-d).

Next, we wondered if cell size (surface area or volume) was a major determinant of centriole abundance. In MTEC cultures, cell size and surface area are established roughly 1-2 days before the ciliogenesis transcriptional program is initiated. This temporal separation provided us with a means to determine whether the centriole amplification machinery responds to the differences in cell size set at the end of the proliferation phase. To test this, we manipulated cell shape and size prior to inducing differentiation by growing basal cells on varying concentrations of extracellular collagen. Modulating extracellular matrix density is a commonly used approach to manipulate cell volume and/or surface area [42-45]. Culture and differentiation of basal cells on increasing concentrations of extracellular collagen resulted in a dose-dependent increase in cell surface area (Fig. 7a-b). Remarkably, centriole abundance also increased in a dose-dependent manner (Fig. 7c). To determine whether the increase in average centriole number per cell was a function of increased cell volume, we measured cell depth (apical-basal distance). Although the cells contained a larger surface area, they were shallower in depth, resulting in a similar overall cell volume (Fig. 7a and d-e). Thus, the size of surface area, but not overall cell volume, appears to dictate centriole abundance during amplification. Finally, we sought to determine whether the higher centriole number in cells with larger surface areas was regulated at the level of the deuterosome. Indeed, cells grown on higher concentrations of collagen formed a higher proportion of deuterosomes per cell on average (Fig. 7f-g). Collectively, these results indicate that a cell-intrinsic surface area-dependent process establishes centriole abundance, potentially by modulating deuterosome number.

Discussion:

In this study, we sought to determine how MCC establish the number of centrioles and cilia that each cell contains. We first tested the relative contributions of the PC and Plk4 to deuterosome formation, centriole amplification, and establishment of centriole number. Loss of PC had no impact on deuterosome formation and function indicating that, although deuterosomes can be nucleated from the original PC [16], their presence is not essential for the *de novo* centriologenesis pathway. In contrast, the average number of procentriole-forming deuterosomes was slightly but significantly higher upon loss of the PC (Fig. 3 and 5). One intriguing possibility for the increase may be that the deuterosome pathway compensates for the loss of PC-derived centrioles by increasing deuterosome-mediated centriole assembly. This is consistent with our observation that cells lacking the PC formed a similar number of centrioles on average when fully mature (Fig. 4-5). Similarly, inhibition of deuterosome formation was shown to result in increased procentriole nucleation by the PC [13], suggesting that these two centriole assembly pathways likely communicate to regulate centriole biogenesis. However, loss of the PC did impact the kinetics of deuterosome formation; they were evident in PC-less cells slightly earlier than control cells, and persisted at stages (e.g. ALI8) when they would normally have disappeared (Fig. 3 and 5). We interpret these data to suggest that, although the PC are not critical for deuterosome biogenesis, they may help to control the timing of their assembly and disassembly. Nonetheless, the overall process of centriole amplification (initiation, growth and maturation) can proceed normally is the absence of PC.

Although Plk4 kinase function was needed for canonical centriole duplication in proliferating basal cells, it was dispensable for post-mitotic centriole amplification. This was somewhat surprising for two reasons: (a) expression levels of Plk4 increase significantly during centriole amplification in MCC [13, 38], suggestive of a role during those stages, and (b) the kinase is essential for initiating procentriole formation in the majority of mammalian cells examined [7, 26]. Nonetheless, depletion of Plk4 did cause a delay in centriologenesis, indicating that the protein itself might be needed for proper progression through the various stages of centriole assembly. This is reminiscent of what was recently described for other kinases involved in coordinating centriole assembly and cell cycle progression in MCC. For example, it was shown that differentiating, non-dividing MCC repurpose the mitotic regulatory circuitry involving CDK1/Plk1/APC-C to control the timely progression of centriole amplification, maturation, and motile ciliogenesis while avoiding reentry into mitosis [46]. Another study found that CDK2, the kinase responsible for G1-S phase transition, was also required in MCC to initiate the motile ciliogenesis program independent of cell cycle progression [47]. Thus,

one possible reason for the elevated Plk4 protein is to coordinate the timing of centriole assembly and maturation in post-mitotic cells. Indeed, we found that MCC lacking Plk4 initiated centriole assembly to the same extent as control cells, were delayed in passage through the growth and maturation phases, but eventually "caught up" (Fig. 5). Importantly, multiciliated cells lacking Plk4 contained the same number of centrioles on average when fully mature at ALI21, further indicating that it is not critical for regulating number per se. Consistent with this observation, overexpression of Plk4 in MTEC (Fig. 5) or in *Xenopus* larvae MCC [12] did not result in increased centriole number. Thus, Plk4 may play a similar role as CDK1/CDK2/Plk1/APC-C, by participating in a temporal regulatory mechanism that mediates passage through the various centriole assembly steps.

Centriole abundance in MCC scales with surface area, a phenomenon we observed in airway tissues *in vivo* and in MTEC cultures *in vitro*. However, it is unclear which of those properties influences the other: does having a larger surface area result in the formation of more centrioles, or does a cell that forms a larger number of centrioles expand its surface area to accommodate them? One advantage of using the MTEC culture system is that the ciliogenesis program initiates roughly 2 days after basal cells have already established their size and surface area at ALI0. Therefore, we could temporally separate these two events. By growing cells on increasing extracellular collagen matrix density during the proliferation phase, we caused the enlargement of cell surface area before the transcriptional ciliogenesis program initiated. Remarkably, we discovered that cells formed more centrioles once fully differentiated, suggesting that the centriole amplification machinery responds to the change in surface area. We attempted the reciprocal experiment, which was to induce the formation of excess centrioles and test whether the size of the surface area changed accordingly. Although constitutive overexpression of Plk4 did result in the formation of excess PC, it did not alter final centriole number or surface area (Fig. 5 and data not shown).

How are the variations in cell surface area communicated to the centriole amplification pathway to establish centriole number? There are at least three possible ways we envision this could occur. First, larger cells might increase transcription of genes essential for centriole and cilia assembly. This would be consistent with the "limiting component" model of organelle abundance [48-50], where a fixed quantity of a precursor protein(s) would be expressed then "used up" as centriole assembly occurs. In this scenario, the number of centrioles assembled would stop once the limiting component is no longer available. We did note an increase in deuterosome number in cells with enlarged surface area (Fig. 7), suggesting that transcriptional output of at least some precursors is

likely elevated. However, it remains unclear whether there is a single limiting component, or if all centriolar proteins become expressed at higher levels in larger cells. Alternatively, cells with larger surface areas might spend a longer period of time in stages of centriole assembly compared to smaller cells. In this scenario, the rate of centriole assembly would be the same in cells of different size, but ones with larger surface areas would spend longer periods in stages I-III to generate more total centrioles. Since the amount of time spent in these assembly stages is coordinated by proteins such as CDK1/Plk1CDK2/APC-C [46, 47], one possibility is that these pathways help relay information about cell surface area/size to the centriole assembly machinery, and fine-tune the length of time spent in assembly to achieve the desired final number. Finally, it is possible that the apical cytoskeleton helps instruct the centriole amplification pathway to regulate centriole abundance per cell. It is well established that an apical actin network in MCC plays a critical role in modulating the surface area, regulating centriole migration and docking at the plasma membrane, ensuring the even distribution of centrioles across the cell surface, and orienting (planar polarization) of centrioles [51-58]. What remains unclear is whether this actin network communicates with the centriole amplification machinery to regulate centriole number. One possibility is that the variations in surface area may result in corresponding changes to the size of the apical actin lattice, which could then instruct the centriologenesis program to generate more centrioles. Our future studies will focus on defining the pathway(s) coordinating the relationship between cell surface area and centriole amplification. These will have important clinical implications for ciliopathies caused by reduced cilia abundance in MCC, such Primary Ciliary Dyskinesia (PCD) and hydrocephalus.

Acknowledgments:

We thank X. Zhu (Shanghai Institutes for Biological Sciences, China) for generously sharing the Deup1 and Plk4 antibodies, N. Da Silva and R. Basto (CNRs, Institut Curie, Paris, France) for providing the *Tg::mChPlk4* mice, Cep152 and Cep135 antibodies, K. Oogema and A.K. Shiau (Ludwig Institute for Cancer Research, La Jolla, CA) for initially sharing the Centrinone compounds. We also thank S. Dutcher, P. Bayly and A. Horani (Washington University in St Louis, MO) for critical reading of the manuscript. We appreciate the comments and feedback on this project from all members of the Washington University Cilia Group. This study was supported by funding from the National Heart, Lung and Blood Institute (NHLBI, R01-HL128370) to M.R.M and S.L.B. The authors declare no competing financial interests.

Online Methods:

Cell culture:

All animal studies were performed following protocols that are compliant with guidelines of the Institutional Animal Care and Use Committee at Washington University and the National Institutes of Health. Mouse Tracheal Epithelial Cell (MTEC) cultures were established as previously described [14, 18, 19, 21]. Briefly, C57BL/6J mice were euthanized at 2-4 months of age, trachea were excised, opened longitudinally to expose the lumen, placed in 1.5 mg/ml pronase E in DMEM/F-12 supplemented with antibiotics and incubated at 4°C overnight. Tracheal epithelial progenitor cells were dislodged by gentle agitation and collected in DMEM/F12 containing 10% FBS. After centrifugation at 4°C for 10 min at 800 g, cells were resuspended in DMEM/F12 with 10% FBS and plated in a Primaria Tissue Culture dish (Corning) for 3-4 h at 37°C with 5% CO_2 to adhere contaminating fibroblasts. Non-adhered cells were collected, concentrated by centrifugation, resuspended in an appropriate volume of MTEC-complete medium (described in [18, 19]), and seeded at a density of $9X10^4$ cells/cm^2 onto Transwell-Clear permeable filter supports (Corning) treated with 0.06mg/ml rat tail Collagen type I. Air liquid interface (ALI) was established after cells reached confluence by feeding cells with MTEC serum-free medium [18, 19] only in the lower chamber. To ablate parental centrioles using Centrinone, cells were incubated in medium supplemented with 1 μM Centrinone A [22] beginning at 2 days after seeding. Cells were cultured at 37°C with 5% CO_2, and media containing Centrinone replaced every 2 days for up to 21 days. Samples were harvested at ALI days 0, 1, 2, 3, 4, 6, 8, 12 and 21, fixed and analyzed as described below. All chemicals were obtained from Sigma-Aldrich unless otherwise indicated. All media were supplemented with 100 U/ml penicillin, 100 mg/ml streptomycin, and 0.25 mg/ml Fungizone (all from Invitrogen).

To induce constitutive overexpression of Plk4 in MTEC, transgenic *Tg::mCherry-Plk4* animals containing a Chloramphenicol Acetyl Transferase (CAT) coding sequence that includes a stop codon flanked by two loxP sites [39, 59] were mated to *Tg::Rosa26-Cre^{ERT2}* mice [41] that conditionally express Cre-recombinase in the majority of tissues. Trachea were isolated from *Tg::mChPlk4-Rosa26-Cre^{ERT2}* and basal progenitor cells isolated as described. Cre-recombinase expression was induced by adding 1 μm 4-hydroxytamoxifen (Sigma) during the proliferation stage, beginning at 2 days post-seeding. Cells were incubated with tamoxifen for a total of 4-6 days up to ALI 0 to induce expression of mChPlk4. Air liquid-interface was established once cells reached full confluence, samples harvested and fixed at ALI days 0, 1, 2, 3, 4, 8, 12 as described above.

Lentivirus production and cell infection:

Two lentivirus-based shRNA constructs targeting mouse Plk4 (shRNA#1: nucleotides 726–747, 5′-GCTTTGACAATCTACCAGAAA -3′; shRNA#2: nucleotides 1896–1917, 5′-CCACCAGTTACTTCGTAGAAA -3′) were used. Plasmids were obtained from the RNAi Consortium (TRC) collection available at the Washington University School of Medicine Hope Center for Neurological Disorders Viral Vectors Core (https://hopecenter.wustl.edu). Lentivirus was produced by co-transfection of HEK293T cells with the appropriate transfer and lentiviral helper plasmids (pCMVDR8.74 and pMD2.VSVG) using Lipofectamine 3000. To infect MTEC, cells were seeded on Transwell filters in the presence of shRNA-expressing lentivirus at an MOI of 1, and infected cells selected with 2μg/mL puromycin for 4-6 days until they reached confluence. ALI was established as described, and samples harvested on the indicated days.

Immunofluorescence:

For immunofluorescence assays MTEC were rinsed twice with PBS and fixed in either 100% ice-cold methanol at −20°C for 10 min, or with 4% paraformaldehyde in PBS at room temperature for 10 min, depending on antigen. Cells were rinsed twice with PBS, filters excised from their plastic supports and cut into quarters to provide multiple equivalent samples for parallel staining. Cells were briefly extracted with 0.2% Triton X-100 in PBS and blocked for 1 h at room temperature with 3% BSA (Sigma) in PBS. Samples were incubated with primary antibodies for 1 h at room temperature or 4°C overnight. Primary antibodies used in the study: Mouse anti-Centrin (clone 20H5; 1:2,000; EMD Millipore 04-1624), rat anti-Cep120 (clone 2; 1:2000; [32]), mouse anti-acetylated α-tubulin (clone 6-11B0-1; 1:5000; Sigma-T6793), rabbit anti-Cep164 (1:1000; [60]), rabbit anti-Cep135 and rabbit anti-Cep152 (1:1000; gift from R. Basto, Institute Curie, Paris, France), rabbit anti-Deup1 (1:400) and rabbit anti-Plk4 (1:200; [13]), mouse anti-Sas6 (1:200; Santa Cruz - sc-81431), rat anti-ZO-1 (1:1000; Santa Cruz sc-33725), rabbit anti-ZO-1 (1:500, Zymed Laboratories Inc - 61-7300). Alexa Fluor dye–conjugated secondary antibodies (Invitrogen) were used at a dilution of 1:500 at room temperature for 1 h. Samples were mounted in Mowiol antifade medium containing N-propyl gallate (Sigma). For whole-mount *in situ* staining, freshly-excised trachea were fixed using 4% paraformaldehyde in PBS at room temperature for 5 min, then ice-cold methanol at −20°C for 5 min. The tissue was washed in PBS, blocked and incubated with primary antibody as described.

Images were captured using a Nikon Eclipse Ti-E inverted confocal microscope equipped with a 60X (1.4 NA) or 100X (1.45 NA) Plan Fluor oil immersion objective lens (Nikon, Melville, NY). A

series of digital optical sections (z-stacks) were captured at 0.2 µm intervals using an Andor Neo-Zyla CMOS camera at room temperature. Three-dimensional superresolution structured illumination microscopy (3D-SIM) images were captured on an inverted Nikon Ti-E microscope using 100X oil objective (1.45 NA) at the Washington University Center for Cellular Imaging. Optical z-sections were separated by 0.216 µm, and 3D-SIM images were processed and reconstructed using the Nikon Elements AR 4 Software.

Electron microscopy:

MTEC grown on Transwell filters were fixed with freshly prepared 2.5% glutaraldehyde in PBS, washed in PBS for 30 min, pre-stained with 2% osmium tetroxide and 1% uranyl acetate, dehydrated in graded ethanol series, and then embedded in Embed 812 resin. Samples were serially sectioned from the cell's apical surface to the basal membrane, above the filter. The thickness of the sections was 80 nm (for ALI3 samples), or 120 (for ALI0 samples). Serial sections were transferred onto formvar coated copper slot grids, stained with 2% uranyl acetate and 0.4% lead citrate, and imaged using a transmission electron microscope (FEI Tecnai T12) operating at 80 kV. The alignment of the serial sections and image analysis was performed in Adobe Photoshop and Fiji (NIH).

Image analysis and measurements:

Quantification of centriole abundance, deuterosome number, surface area and volume were performed using Nikon Elements AR 4 Software. To determine the extent of parental centriole loss, cells at ALI 0 were scored for centriole number (0, 1, 2, 3, 4 centrioles) per cell. To determine the fraction of cells in the population undergoing centriole amplification during differentiation, cells at ALI 1, 2, 3, 4 and 8 were scored for the presence of centriolar aggregates (Agg.), which then become defined as multiciliated cells (MCC). This approach was applied to each centriolar marker, and the percentage of the population undergoing centriole amplification determined. The surface area was defined by staining cells with ZO-1 to mark the apical cell-cell junctions, and measured using the thresholding algorithm (Elements AR 4). Cells were binned into three categories that ranged from what we define as small (<50 μm^2), medium (50-100 μm^2) and large (>100 μm^2). Cell volume was determined by measuring the apical-basal distance (depth), which was then multiplied by the surface area. To quantify deuterosome number, MCC at ALI 3-4 were stained for markers of the deuterosome and procentrioles. The number of procentriole-forming deuterosome rings/rosettes

were scored and compared in cells of similar size. To determine the number of centrioles per cell in mature MCC at ALI12 or 21, the spot detection tool (Elements AR 4) with a spot circular ROI of 0.26 µm was used. Centriole abundance was then grouped based on cell size as described. Centrioles density was determined by dividing the number of centrioles per cell by the surface area.

Manipulation of cell surface area:

Freshly isolated basal cells were seeded onto Transwell filters coated with varying concentrations (from 0.06mg/mL – 2.4mg/mL) of type 1 rat tail collagen. Cells were cultured for 4-6 days until confluent then ALI established. Samples were fixed on the indicated days as analyzed for centriole number, surface area and volume. We found that the size of the surface area did not increase significantly beyond 1.2mg/mL collagen concentration, thus we set that value as the upper limit for all subsequent analyses.

Statistical analyses:

Statistical analyses were performed using GraphPad PRISM 7.0 or Microsoft Excel. The vertical segments in box plots show the first quartile, median, and third quartile. The whiskers on both ends represent the maximum and minimum values for each dataset analyzed. For bar graphs, data are reported as mean ± SEM. Collected data were examined by two-tail unpaired Student's t-test. Statistical significance was set at $p < 0.05$.

References:

1. Brooks, E.R. & Wallingford, J.B. Multiciliated cells. *Current biology : CB* **24**, R973-982 (2014).
2. Spassky, N. & Meunier, A. The development and functions of multiciliated epithelia. *Nature reviews. Molecular cell biology* **18**, 423-436 (2017).
3. Amirav, I. *et al.* Systematic Analysis of CCNO Variants in a Defined Population: Implications for Clinical Phenotype and Differential Diagnosis. *Human mutation* **37**, 396-405 (2016).
4. Nunez-Olle, M. *et al.* Constitutive Cyclin O deficiency results in penetrant hydrocephalus, impaired growth and infertility. *Oncotarget* **8**, 99261-99273 (2017).
5. Wallmeier, J. *et al.* Mutations in CCNO result in congenital mucociliary clearance disorder with reduced generation of multiple motile cilia. *Nature genetics* **46**, 646-651 (2014).
6. Boon, M. *et al.* MCIDAS mutations result in a mucociliary clearance disorder with reduced generation of multiple motile cilia. *Nature communications* **5**, 4418 (2014).
7. Nigg, E.A. & Holland, A.J. Once and only once: mechanisms of centriole duplication and their deregulation in disease. *Nature reviews. Molecular cell biology* **19**, 297-312 (2018).
8. Sorokin, S.P. Reconstructions of centriole formation and ciliogenesis in mammalian lungs. *Journal of cell science* **3**, 207-230 (1968).
9. Vladar, E.K. & Stearns, T. Molecular characterization of centriole assembly in ciliated epithelial cells. *The Journal of cell biology* **178**, 31-42 (2007).
10. Steinman, R.M. An electron microscopic study of ciliogenesis in developing epidermis and trachea in the embryo of Xenopus laevis. *The American journal of anatomy* **122**, 19-55 (1968).
11. Kalnins, V.I. & Porter, K.R. Centriole replication during ciliogenesis in the chick tracheal epithelium. *Zeitschrift fur Zellforschung und mikroskopische Anatomie* **100**, 1-30 (1969).
12. Klos Dehring, D.A. *et al.* Deuterosome-mediated centriole biogenesis. *Developmental cell* **27**, 103-112 (2013).
13. Zhao, H. *et al.* The Cep63 paralogue Deup1 enables massive de novo centriole biogenesis for vertebrate multiciliogenesis. *Nature cell biology* **15**, 1434-1444 (2013).
14. Mahjoub, M.R., Xie, Z. & Stearns, T. Cep120 is asymmetrically localized to the daughter centriole and is essential for centriole assembly. *The Journal of cell biology* **191**, 331-346 (2010).
15. Tang, T.K. Centriole biogenesis in multiciliated cells. *Nature cell biology* **15**, 1400-1402 (2013).

16. Al Jord, A. *et al.* Centriole amplification by mother and daughter centrioles differs in multiciliated cells. *Nature* **516**, 104-107 (2014).
17. Vladar, E.K. & Brody, S.L. Analysis of ciliogenesis in primary culture mouse tracheal epithelial cells. *Methods in enzymology* **525**, 285-309 (2013).
18. You, Y. & Brody, S.L. Culture and differentiation of mouse tracheal epithelial cells. *Methods in molecular biology* **945**, 123-143 (2013).
19. You, Y., Richer, E.J., Huang, T. & Brody, S.L. Growth and differentiation of mouse tracheal epithelial cells: selection of a proliferative population. *American journal of physiology. Lung cellular and molecular physiology* **283**, L1315-1321 (2002).
20. Habedanck, R., Stierhof, Y.-D., Wilkinson, C.J. & Nigg, E.A. The Polo kinase Plk4 functions in centriole duplication. *Nature cell biology* **7**, 1140-1146 (2005).
21. Silva, E. *et al.* Ccdc11 is a novel centriolar satellite protein essential for ciliogenesis and establishment of left-right asymmetry. *Molecular biology of the cell* **27**, 48-63 (2016).
22. Wong, Y.L. *et al.* Cell biology. Reversible centriole depletion with an inhibitor of Polo-like kinase 4. *Science* **348**, 1155-1160 (2015).
23. Arquint, C. & Nigg, E.A. The PLK4-STIL-SAS-6 module at the core of centriole duplication. *Biochemical Society transactions* **44**, 1253-1263 (2016).
24. Bettencourt-Dias, M. *et al.* SAK/PLK4 is required for centriole duplication and flagella development. *Current biology : CB* **15**, 2199-2207 (2005).
25. Pearson, C.G. & Winey, M. Plk4/SAK/ZYG-1 in the regulation of centriole duplication. *F1000 Biol Rep* **2**, 58 (2010).
26. Sillibourne, J.E. & Bornens, M. Polo-like kinase 4: the odd one out of the family. *Cell Div* **5**, 25 (2010).
27. Holland, A.J., Lan, W., Niessen, S., Hoover, H. & Cleveland, D.W. Polo-like kinase 4 kinase activity limits centrosome overduplication by autoregulating its own stability. *The Journal of cell biology* **188**, 191-198 (2010).
28. Cizmecioglu, O. *et al.* Cep152 acts as a scaffold for recruitment of Plk4 and CPAP to the centrosome. *The Journal of cell biology* **191**, 731-739 (2010).
29. Dammermann, A. *et al.* Centriole assembly requires both centriolar and pericentriolar material proteins. *Developmental cell* **7**, 815-829 (2004).
30. Hatch, E.M., Kulukian, A., Holland, A.J., Cleveland, D.W. & Stearns, T. Cep152 interacts with Plk4 and is required for centriole duplication. *The Journal of cell biology* **191**, 721-729 (2010).

31. Kleylein-Sohn, J. *et al.* Plk4-induced centriole biogenesis in human cells. *Developmental cell* **13**, 190-202 (2007).
32. Betleja, E., Nanjundappa, R., Cheng, T. & Mahjoub, M.R. A novel Cep120-dependent mechanism inhibits centriole maturation in quiescent cells. *eLife* **7** (2018).
33. Comartin, D. *et al.* CEP120 and SPICE1 cooperate with CPAP in centriole elongation. *Current biology : CB* **23**, 1360-1366 (2013).
34. Paoletti, A., Moudjou, M., Paintrand, M., Salisbury, J.L. & Bornens, M. Most of centrin in animal cells is not centrosome-associated and centrosomal centrin is confined to the distal lumen of centrioles. *Journal of cell science* **109 (Pt 13)**, 3089-3102 (1996).
35. Stearns, T., Evans, L. & Kirschner, M. Gamma-tubulin is a highly conserved component of the centrosome. *Cell* **65**, 825-836 (1991).
36. Xie, Z. *et al.* Cep120 and TACCs control interkinetic nuclear migration and the neural progenitor pool. *Neuron* **56**, 79-93 (2007).
37. Graser, S. *et al.* Cep164, a novel centriole appendage protein required for primary cilium formation. *The Journal of cell biology* **179**, 321-330 (2007).
38. Hoh, R.A., Stowe, T.R., Turk, E. & Stearns, T. Transcriptional program of ciliated epithelial cells reveals new cilium and centrosome components and links to human disease. *PloS one* **7**, e52166 (2012).
39. Dionne, L.K. *et al.* Centrosome amplification disrupts renal development and causes cystogenesis. *The Journal of cell biology* **217**, 2485-2501 (2018).
40. Marthiens, V. *et al.* Centrosome amplification causes microcephaly. *Nature cell biology* **15**, 731-740 (2013).
41. Ventura, A. *et al.* Restoration of p53 function leads to tumour regression in vivo. *Nature* **445**, 661-665 (2007).
42. Plant, A.L., Bhadriraju, K., Spurlin, T.A. & Elliott, J.T. Cell response to matrix mechanics: focus on collagen. *Biochimica et biophysica acta* **1793**, 893-902 (2009).
43. Trappmann, B. & Chen, C.S. How cells sense extracellular matrix stiffness: a material's perspective. *Current opinion in biotechnology* **24**, 948-953 (2013).
44. Califano, J.P. & Reinhart-King, C.A. Substrate Stiffness and Cell Area Predict Cellular Traction Stresses in Single Cells and Cells in Contact. *Cellular and molecular bioengineering* **3**, 68-75 (2010).
45. Wells, R.G. The role of matrix stiffness in regulating cell behavior. *Hepatology* **47**, 1394-1400 (2008).

46. Al Jord, A. *et al.* Calibrated mitotic oscillator drives motile ciliogenesis. *Science* **358**, 803-806 (2017).
47. Vladar, E.K. *et al.* Cyclin-dependent kinase control of motile ciliogenesis. *eLife* **7** (2018).
48. Goehring, N.W. & Hyman, A.A. Organelle growth control through limiting pools of cytoplasmic components. *Current biology : CB* **22**, R330-339 (2012).
49. Marshall, W.F. Cell Geometry: How Cells Count and Measure Size. *Annual review of biophysics* **45**, 49-64 (2016).
50. Chan, Y.H. & Marshall, W.F. How cells know the size of their organelles. *Science* **337**, 1186-1189 (2012).
51. Kulkarni, S.S., Griffin, J.N., Date, P.P., Liem, K.F., Jr. & Khokha, M.K. WDR5 Stabilizes Actin Architecture to Promote Multiciliated Cell Formation. *Developmental cell* **46**, 595-610 e593 (2018).
52. Mahuzier, A. *et al.* Ependymal cilia beating induces an actin network to protect centrioles against shear stress. *Nature communications* **9**, 2279 (2018).
53. Sedzinski, J., Hannezo, E., Tu, F., Biro, M. & Wallingford, J.B. RhoA regulates actin network dynamics during apical surface emergence in multiciliated epithelial cells. *Journal of cell science* **130**, 420-428 (2017).
54. Herawati, E. *et al.* Multiciliated cell basal bodies align in stereotypical patterns coordinated by the apical cytoskeleton. *The Journal of cell biology* **214**, 571-586 (2016).
55. Antoniades, I., Stylianou, P. & Skourides, P.A. Making the connection: ciliary adhesion complexes anchor basal bodies to the actin cytoskeleton. *Developmental cell* **28**, 70-80 (2014).
56. Werner, M.E. *et al.* Actin and microtubules drive differential aspects of planar cell polarity in multiciliated cells. *The Journal of cell biology* **195**, 19-26 (2011).
57. Sedzinski, J., Hannezo, E., Tu, F., Biro, M. & Wallingford, J.B. Emergence of an Apical Epithelial Cell Surface In Vivo. *Developmental cell* **36**, 24-35 (2016).
58. Pan, J., You, Y., Huang, T. & Brody, S.L. RhoA-mediated apical actin enrichment is required for ciliogenesis and promoted by Foxj1. *Journal of cell science* **120**, 1868-1876 (2007).
59. Marthiens, V., Piel, M. & Basto, R. Never tear us apart--the importance of centrosome clustering. *Journal of cell science* **125**, 3281-3292 (2012).
60. Firat-Karalar, E.N., Sante, J., Elliott, S. & Stearns, T. Proteomic analysis of mammalian sperm cells identifies new components of the centrosome. *Journal of cell science* **127**, 4128-4133 (2014).

Figure Legends:

Figure 1 – Parental centrioles are dispensable for centriole amplification. (a) Schematic of the proliferation and differentiation steps of multiciliated respiratory epithelia. The key stages of centriole amplification from parental centrioles and deuterosomes are depicted. **(b)** Immunofluorescence (3D-SIM) images of control and Centrinone-treated cells. Samples were fixed on the indicated days of air-liquid interface (ALI) culture and stained for centrioles (centrin) and apical cell-cell junctions (ZO-1). Upper panels show lower magnification images, and lower panels highlight a single cell. Scale bar = 10 μm. **(c)** Quantification of centriole number, and the fraction of the population undergoing centriole amplification, in control and Centrinone-treated MTEC. Ablation of parental centrioles did not affect the initiation of centriolar aggregate (Agg.) formation, the timing of centriole amplification, or the fraction of mature multiciliated cells (MCC) in the population. Results are averages of three independent experiments. More than 3,000 cells were counted per sample for each time point. * $p<0.05$. **(d)** Transmission electron microscopy (TEM) of the apical surface of MTEC at ALI0. Parental centrioles were easily found at the apical surface of control cells (20/20 cells examined; insets highlight three sets of PC), but were missing in the majority of Centrinone-treated samples (0 parental centrioles in 17/19 cells). Scale bars = 2 μm (large panels) and 400 nm (insets).

Figure 2 – Loss of parental centrioles does not affect dynamics of centriole amplification. (a) Immunofluorescence images of control and Centrinone-treated cells. Samples were fixed on the indicated days and stained for Plk4, centrioles (γ-tubulin) and apical cell-cell junctions (ZO-1). Upper panels show lower magnification images, and lower panels highlight a single cell. Inhibition of Plk4 kinase activity results in accumulation of Plk4 protein at ALI 0-1, and the protein is still evident at stages (e.g. ALI 8) when it is normally lost. Scale bar = 10 μm. **(b)** Quantification of the fraction of Plk4-expressing cells during differentiation. Results are averages of two independent experiments. More than 1,500 cells were counted per sample for each time point. * $p<0.05$. **(c)** Quantification of the fraction of Sas6-expressing cells during differentiation. A slight increase in Sas6-expressing cells is evident at ALI 0-1 in Centrinone-treated samples, however the overall pattern of expression is not affected. Results are averages of two independent experiments. More than 1000 cells were counted per sample for each time point. * $p<0.05$. **(d-g)** Quantification of centriole number and the fraction of the population undergoing centriole amplification. Cells at the indicated time points were stained for markers of procentriole initiation **(**d and e) and centriole growth (f and g). Ablation of parental

centrioles did not affect the formation of centriolar aggregates (Agg.), the timing of centriole amplification and growth, or the fraction of mature multiciliated cells (MCC) in the population. Results are averages of two independent experiments. More than 2000 cells were counted per sample for each time point. * $p<0.05$.

Figure 3 – Deuterosome biogenesis is unaffected by loss of parental centrioles. (a) Immunofluorescence images of control and Centrinone-treated cells stained with antibodies against deuterosomes (Deup1), centrioles (γ-tubulin) and apical cell-cell junctions (ZO-1). Upper panels show lower magnification images, and lower panels highlight a single cell. Loss of PC does not disrupt deuterosome formation. In contrast, they appear earlier than in control cells (e.g. ALI 1) and persist for a longer period of time. Scale bar = 10 μm. **(b)** Quantification of the fraction of Deup1-expressing cells during differentiation. Results are averages of two independent experiments. More than 1000 cells were counted per sample for each time point. * $p<0.05$. **(c)** 3D-SIM images of MTEC at ALI stained for deuterosomes (Deup1), procentrioles (Sas6) and apical cell-cell junctions (ZO-1). Scale bar = 10 μm. **(d)** Quantification of deuterosome number in control and Centrinone-treated cells. Cells were grouped based on the size of their surface area, and the average number of deuterosomes per cell determined. Loss of PC causes an increase in deuterosome number in each category. N = 87 (control) and 71 (Centrinone). * $p<0.05$. **(e)** TEM images of control and Centrinone-treated MTEC at ALI3, confirming the presence of procentriole-forming deuterosomes that appear normal in size and morphology. Scale bars = 2 μm (upper panels) and 800 nm (magnified lower panels).

Figure 4 – Centriole abundance correlates with surface area and is unaffected by loss of PC. (a) Example 3D-SIM images of mature multiciliated cells at ALI12 stained with markers of centrioles (centrin) and apical cell junctions (ZO-1). Scale bar = 10 μm. (**b-c)** Quantification of centriole number in control cells shows a linear relationship with cell surface area, such that larger cells contain more centrioles. Loss of the PC following Centrinone-treatment does not affect this relationship. **(d-e)** Comparison of abundance and density in mature MCC of varying sizes at ALI12. Loss of the PC did not result in a decrease in average centriole number (d). In fact, there was a slight increase in some cells. Similarly, the density and distribution of these centrioles at the apical surface was generally unchanged (e), although we noted a small but significant increase in the density of centrioles, possibly due to the elevated number per cell. Results are averages of two independent experiments. N = 55 (control) and 60 (Centrinone). * $p<0.05$.

Figure 5 – Depletion of Plk4 causes a delay in centriologenesis but does not affect abundance. (a) Images of MTEC infected with control or Plk4-targeting shRNA. Cells were fixed on the indicated days and stained for centrioles (centrin), endogenous Plk4, procentrioles (Sas6 or centrin), deuterosomes (Deup1) and apical cell junctions (ZO-1). Scale bar = 10μm. **(b)** Depletion of Plk4 in basal cells causes loss of parental centrioles by ALI0, quantified using centrin staining of PC (a). Results are averages of three independent experiments. N = 862 (control shRNA), 846 (Plk4 shRNA1) and 1,108 (Plk4 shRNA2). * $p<0.05$. **(c-d)** Fraction of MCC at ALI3 undergoing centriole amplification in the absence of Plk4. The percentage of cells that initiated centriole amplification, determined using Deup1 and centrin staining, was unchanged (d). However, there was a large decrease in the fraction of MCC with detectable Plk4 (c). Results are averages of two independent experiments. N = 4,158 (control shRNA), 1,596 (Plk4 shRNA1) and 3,456 (Plk4 shRNA2). * $p<0.05$. **(e)** Quantification of deuterosome number in control and Plk4-depleted cells. Similar to Centrinone-mediated PC loss, the number of deuterosomes per cell increases in the absence of PC. Results are averages of two independent experiments. N = 43 (control shRNA), 59 (Plk4 shRNA1) and 67 (Plk4 shRNA2) cells. * $p<0.05$. **(f-g)** Comparison of centriole amplification stages upon Plk4 depletion at ALI12 (f) and ALI21 (g). Although the proportion of the MCC in the population was unchanged in cells lacking Plk4, a significant fraction of the cells were in Stage I-II (with Deup1-positive deuterosomes still evident) and Stage III-IV (absence of deuterosomes) of centriole amplification (f). Culturing the cells for an additional 9 days (ALI21) resulted in an increase in the percentage of mature MCC with cilia in Plk4-depleted cells (g), highlighting a delay in the maturation process. Results are averages of two independent experiments. N = 815 (control shRNA), 783 (Plk4 shRNA1) and 1,346 (Plk4 shRNA2). * $p<0.05$. **(h)** Comparison of centriole abundance in control and Plk4-depleted mature MCC at ALI21. Loss of Plk4 and PC did not result in a decrease in average centriole number. N = 43 (control shRNA), 57 (Plk4 shRNA1) and 67 (Plk4 shRNA2). * $p<0.05$. **(i)** 3D-SIM images of MTEC generated from *Tg::mChPlk4/Rosa26-Cre*^{ERT2} (described in detail in Methods), stained for exogenous Plk4 (mCherry), centrioles (centrin) and apical cell junctions (ZO-1). Addition of tamoxifen during proliferation resulted in constitutive overexpression of mChPlk4,and caused formation of supernumerary PC by ALI0. Importantly, the protein was continuously expressed and still evident in fully mature MCC at ALI12. Scale bar = 10 μm. **(j)** Supernumerary parental centrioles and constitutive overexpression of Plk4 do not result in increased centriole abundance in mature MCC. Results are averages of two independent experiments. N = 31(-TAM), and 30 (+TAM).

Figure 6 – Centriole abundance correlates with surface area *in vivo*. (a) Example 3D-SIM image of adult mouse trachea (P60) immunostained for centrioles (centrin) and apical cell junctions (ZO-1). Scale bar = 10 μm. **(b-d)** Centriole number ranges between 100-400 per cell on average and displays a liner relationship with surface area, consistent with the observations in MTEC. Similarly, centriole density decreases slightly as surface area increases. N = 95 cells.

Figure 7 – Enlargement of the surface area of progenitor cells results in increased centriole abundance. (a) Example 3D-SIM images of MTEC grown on varying concentrations of extracellular collagen matrix. Top panels show X-Y orientation, and lower panels the X-Z dimension. Scale bar = 10 μm. **(b-e)** Analysis of surface area (b), centriole number (c), apical-basal distance (depth, d) and cell volume (e) in MTEC cultured on differing concentrations of collagen. Increasing the collagen density resulted in a dose-dependent expansion of the apical surface, whereas the cells became shallower, resulting in a similar overall cell volume. Importantly, the increase in surface are at ALI0 resulted in increased centriole number (c). Results are averages of two independent experiments. N = 39 (0.06mg/mL), 48 (0.6mg/mL) and 42 (1.2mg/mL). * $p<0.05$. **(f)** 3D-SIM images of MTEC grown on normal (0.06mg/mL) and high (1.2mg/mL) levels of extracellular collagen. Cells at ALI3 were immunostained with antibodies to mark deuterosomes (Deup1), procentrioles (Sas6) and apical cell junctions (ZO-1). Scale bar = 10 μm. (g) Quantification of deuterosome number in MTEC at ALI3 showed a significant increase in cells grown on increased collagen density (with larger surface areas). Results are averages of two independent experiments. N = 45 (0.06mg/mL) and 43 (1.2mg/mL). * $p<0.05$.

Supplementary Figure Legends:

Supplementary Figure 1 – Analysis of procentriole assembly in control and Centrinone-treated MTEC. Immunofluorescence images of control and Centrinone-treated cells. Samples were fixed on the indicated days and stained for markers of parental centrioles and early procentriole nucleation as follows: **(a)** centrin and Sas6, **(b)** Cep152, and **(c)** Cep135 and γ-Tubulin. Apical cell-cell junctions were marked using ZO-1. Scale bars = 10 μm.

Supplementary Figure 2 – Analysis of procentriole growth in control and Centrinone-treated MTEC. Immunofluorescence images of control and Centrinone-treated cells. Samples were fixed on

the indicated days and stained for markers of parental centrioles and procentriole growth as follows: **(a)** Cep120 and **(b)** γ-Tubulin. Apical cell-cell junctions were marked using ZO-1 or E-cadherin. Scale bars = 10 μm.

Supplementary Figure 3 – Analysis of centriole maturation and ciliogenesis in control and Centrinone-treated MTEC. (a) 3D-SIM images of MTEC at ALI0 and 12 stained for a marker of mature centrioles (distal appendage marker Cep164), centrioles (centrin), and apical cell junctions (ZO-1). Control cells at ALI0 contain a single mature centriole as expected, and these are missing in Centrinone-treated samples lacking the PC. Examination of cells at ALI12 showed no deleterious effects on centriole maturation. Scale bars = 10 μm. **(b)** Quantification of mature centrioles, and the fraction of the population undergoing centriole maturation, in control and Centrinone-treated MTEC. Ablation of parental centrioles did not affect the timing of centriole maturation. Results are averages of two independent experiments. More than 2000 cells were counted per sample for each time point. * $p<0.05$. **(c-d)** Immunofluorescence images of control and Centrinone-treated MTEC at ALI12 stained for cilia (acetylated tubulin) and cell-cell junctions (E-cadherin). Loss of parental centrioles does not disrupt ciliogenesis, further indicating that centriole maturation is unperturbed upon PC loss. Results are averages of three independent experiments. N = 3,000 (control) and 3,000 (Centrinone).

Supplementary Video 1 – Centrinone-mediated inhibition of Plk4 results in loss of parental centrioles at ALI0. Samples were serially sectioned from at the cell's apical surface until the basal membrane above the filter. The thickness of each section was 120 nm. Serial sections were imaged using a transmission electron microscope, and images aligned using Adobe Photoshop and Fiji software. Sections within first 2 μm are shown to illustrate the absence of parental centrioles, which are evident in control cells at or near the apical surface. Scale bar = 4μm.

Figure 1

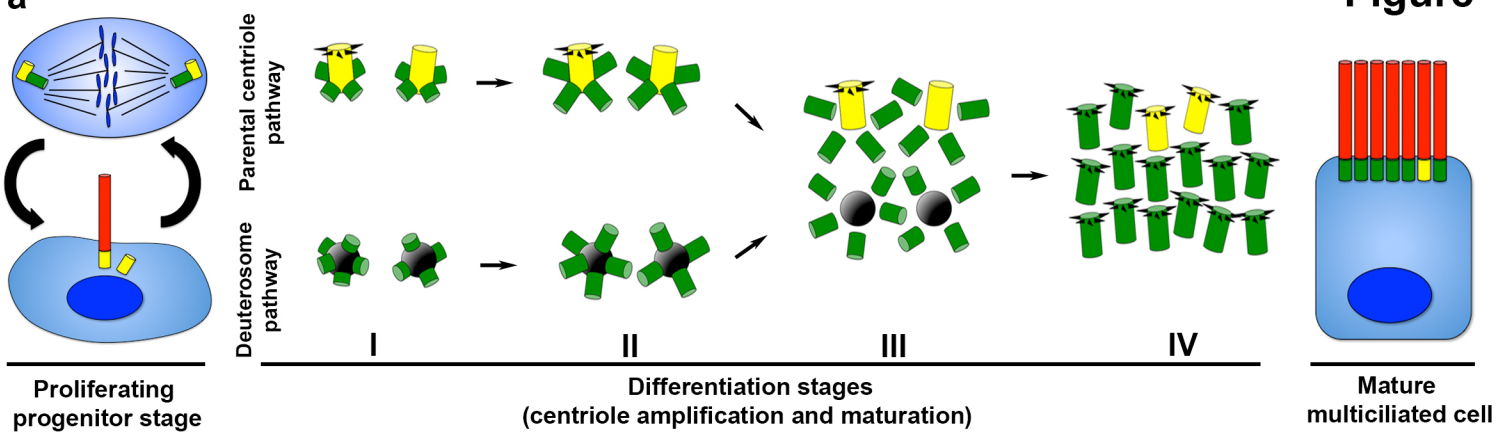
a
Parental centriole pathway
Deuterosome pathway
I
II
III
IV
Proliferating progenitor stage
Differentiation stages (centriole amplification and maturation)
Mature multiciliated cell

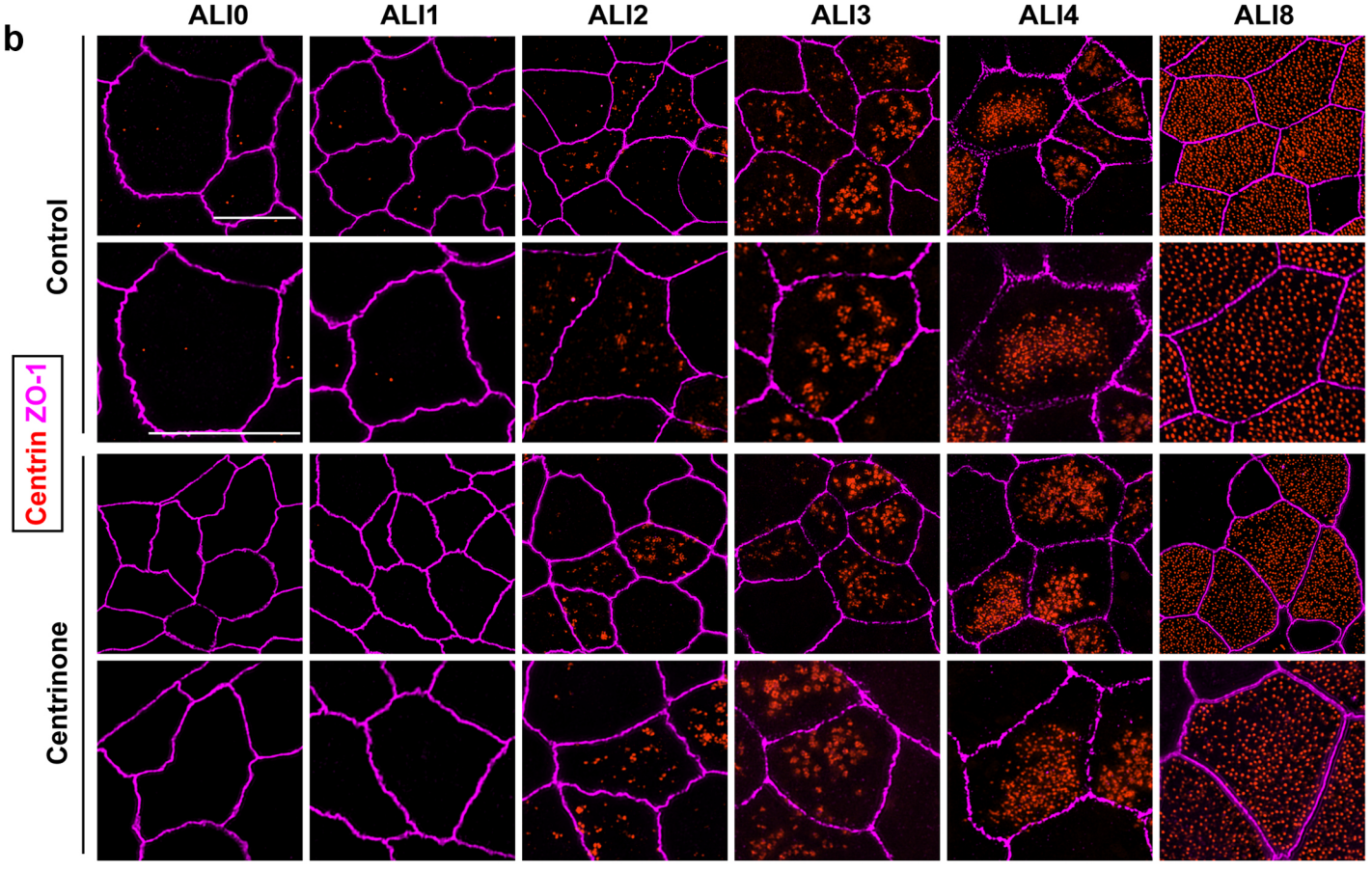
b
ALI0
ALI1
ALI2
ALI3
ALI4
ALI8
Control
Centrinone
Centrin ZO-1

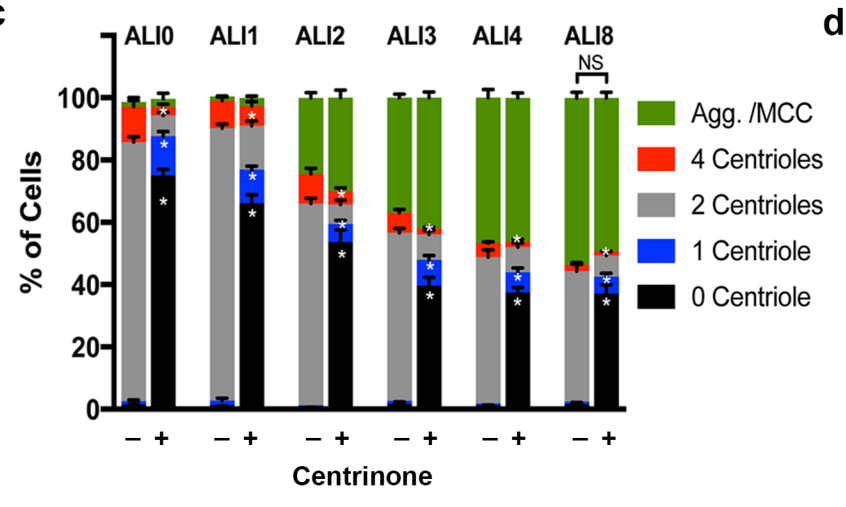
c
ALI0
ALI1
ALI2
ALI3
ALI4
ALI8
NS
% of Cells
100
80
60
40
20
0
– +
Centrinone
Agg. /MCC
4 Centrioles
2 Centrioles
1 Centriole
0 Centriole

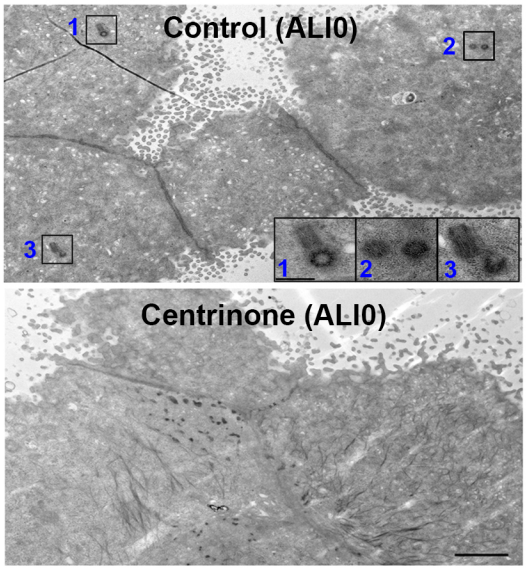
d
Control (ALI0)
Centrinone (ALI0)
1
2
3

Figure 2

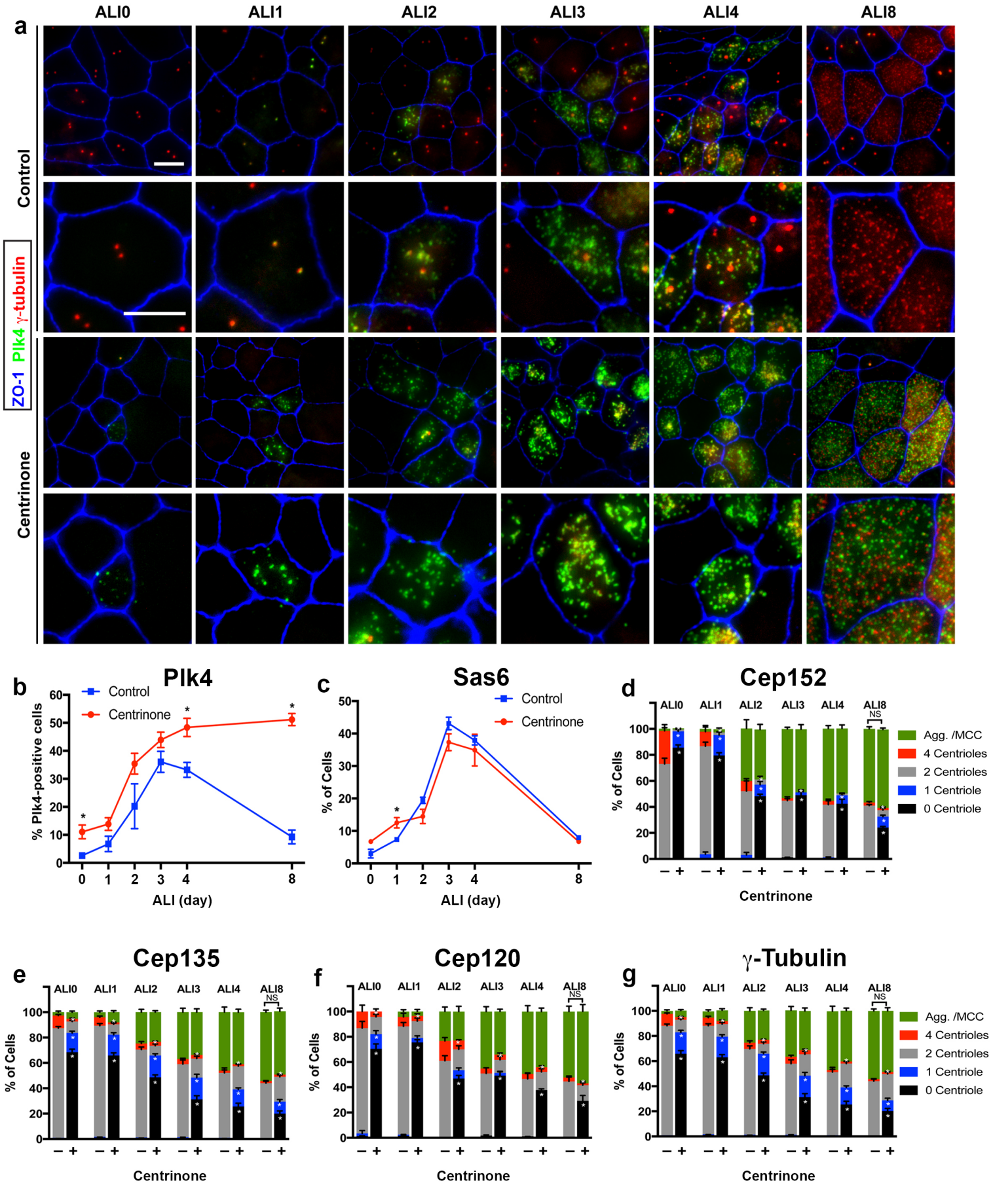
a
ALI0
ALI1
ALI2
ALI3
ALI4
ALI8
Control
Centrinone
ZO-1 Plk4 γ-tubulin
b
Plk4
Control
Centrinone
% Plk4-positive cells
ALI (day)
c
Sas6
Control
Centrinone
% of Cells
ALI (day)
d
Cep152
% of Cells
Agg. /MCC
4 Centrioles
2 Centrioles
1 Centriole
0 Centriole
NS
Centrinone
e
Cep135
f
Cep120
g
γ-Tubulin

Figure 3

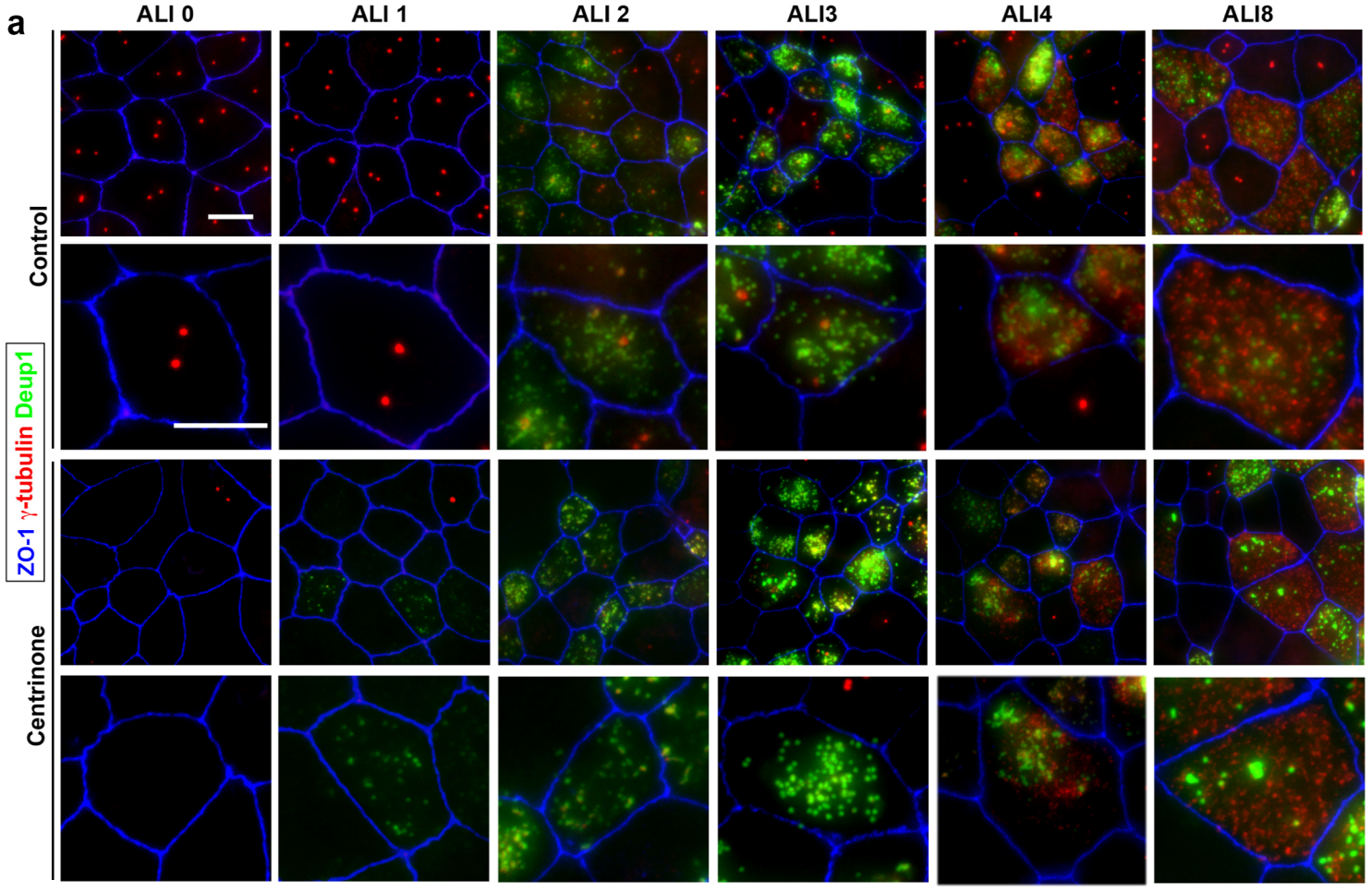
a
ALI 0
ALI 1
ALI 2
ALI3
ALI4
ALI8
Control
Centrinone
ZO-1 γ-tubulin Deup1

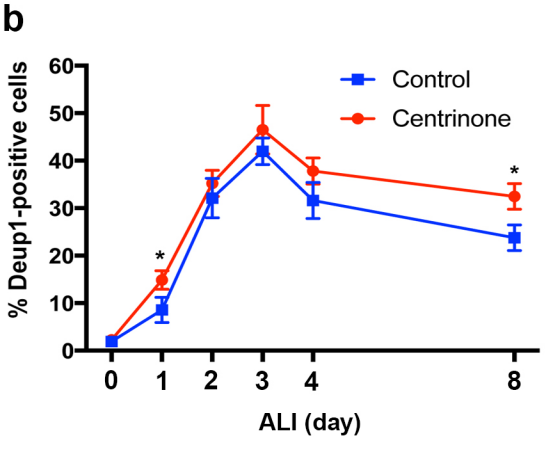
b
% Deup1-positive cells
Control
Centrinone
ALI (day)

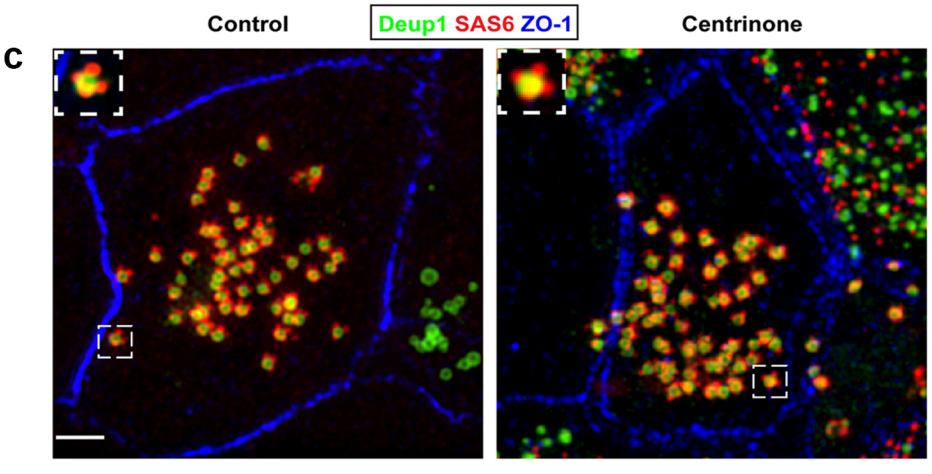
c
Control
Deup1 SAS6 ZO-1
Centrinone

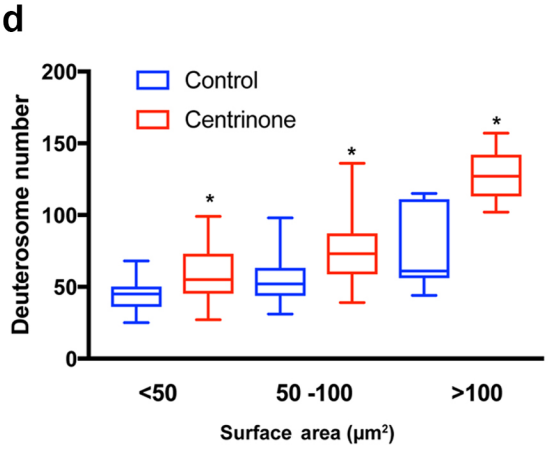
d
Deuterosome number
Control
Centrinone
<50
50 -100
>100
Surface area (μm²)

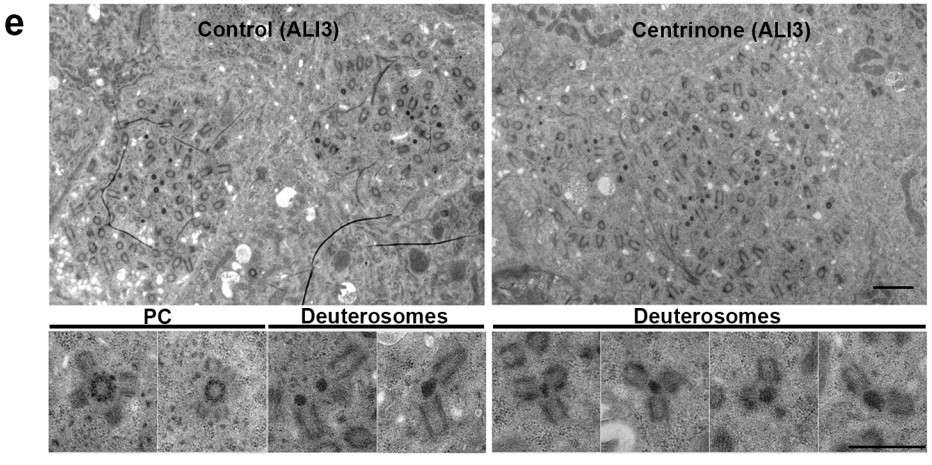
e
Control (ALI3)
Centrinone (ALI3)
PC
Deuterosomes
Deuterosomes

Figure 4

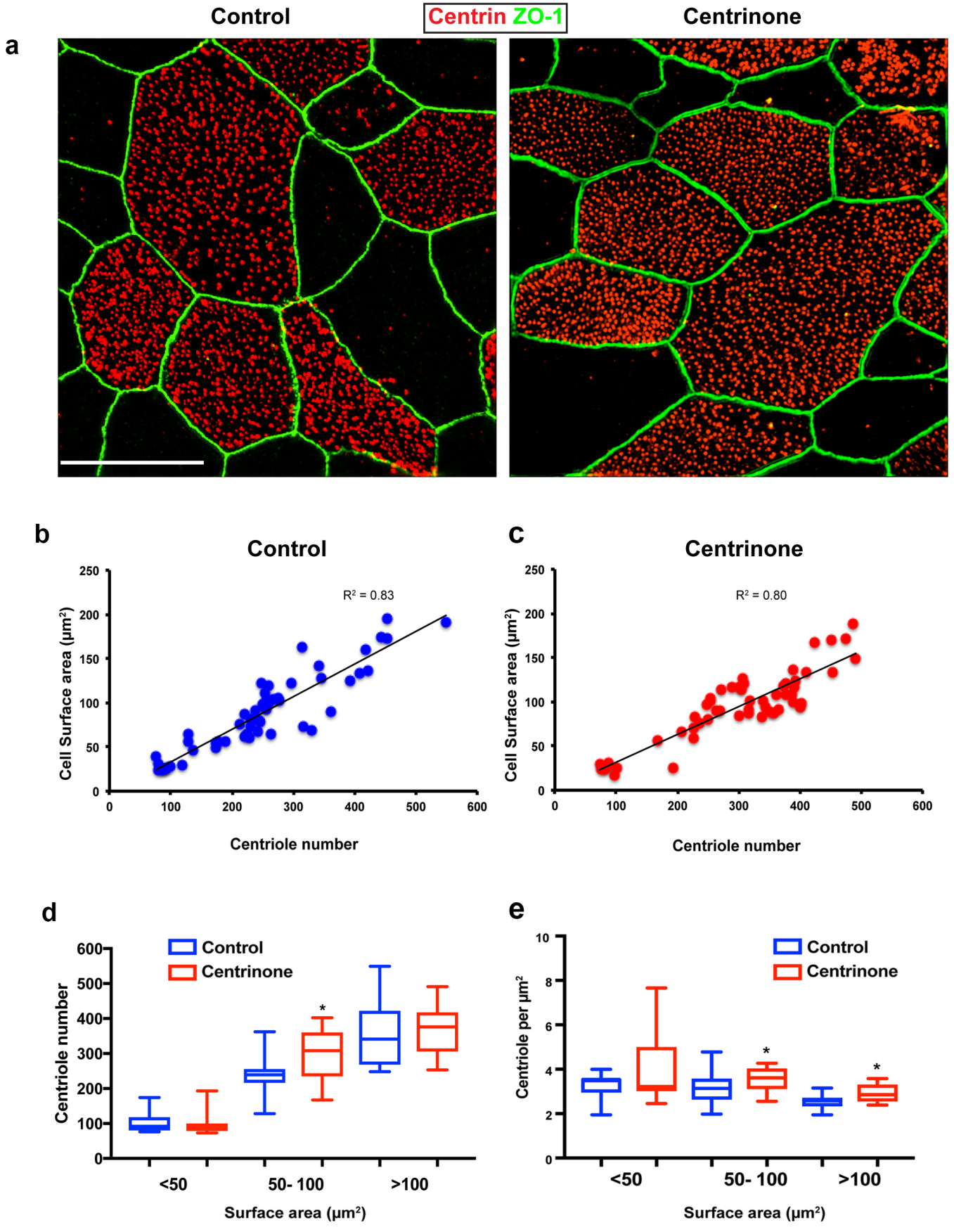
a
Control
Centrin ZO-1
Centrinone
b
Control
R² = 0.83
Cell Surface area (µm²)
Centriole number
c
Centrinone
R² = 0.80
Cell Surface area (µm²)
Centriole number
d
Control
Centrinone
Centriole number
<50
50- 100
>100
Surface area (µm²)
e
Control
Centrinone
Centriole per µm²
<50
50- 100
>100
Surface area (µm²)

Figure 5

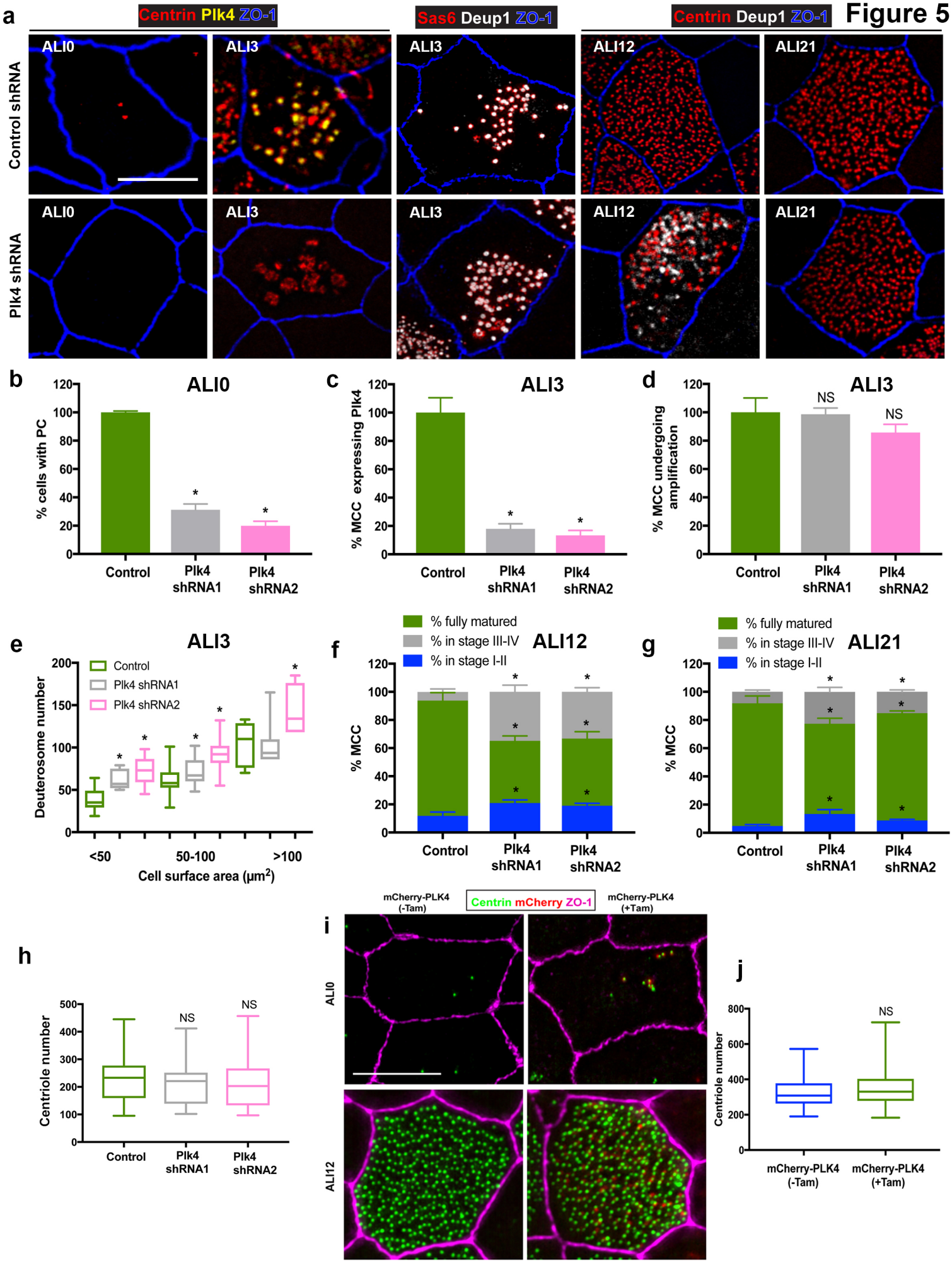
a
Centrin Plk4 ZO-1
Sas6 Deup1 ZO-1
Centrin Deup1 ZO-1
Control shRNA
Plk4 shRNA
ALI0
ALI3
ALI12
ALI21
b
ALI0
% cells with PC
Control
Plk4 shRNA1
Plk4 shRNA2
c
ALI3
% MCC expressing Plk4
d
ALI3
% MCC undergoing amplification
NS
e
ALI3
Control
Plk4 shRNA1
Plk4 shRNA2
Deuterosome number
<50
50-100
>100
Cell surface area (μm²)
f
% fully matured
% in stage III-IV
% in stage I-II
ALI12
% MCC
g
ALI21
h
Centriole number
i
mCherry-PLK4 (-Tam)
Centrin mCherry ZO-1
mCherry-PLK4 (+Tam)
j
Centriole number

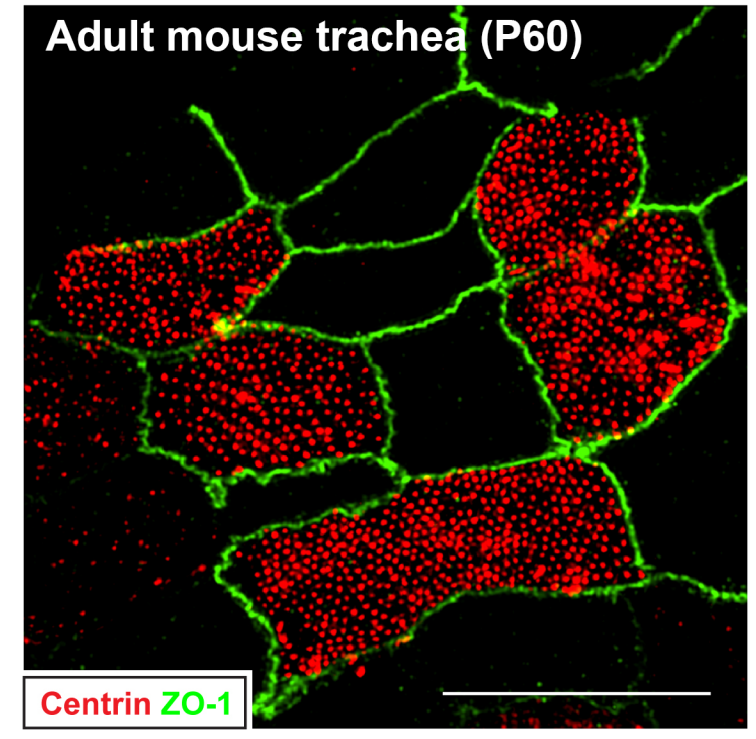
a
Adult mouse trachea (P60)
Centrin ZO-1

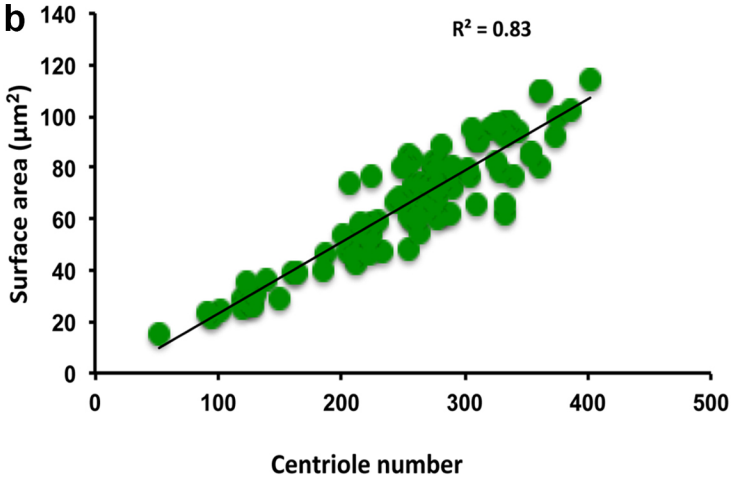
b
R² = 0.83
Surface area (µm²)
Centriole number
0
20
40
60
80
100
120
140
0
100
200
300
400
500

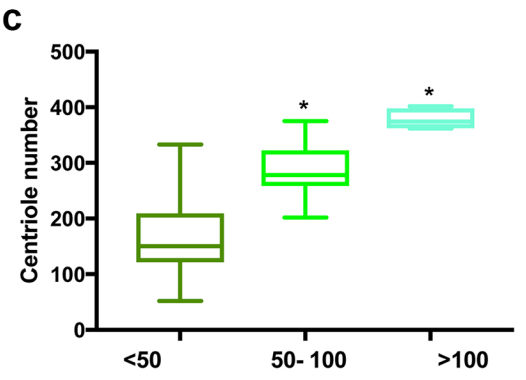
c
Centriole number
0
100
200
300
400
500
*
*
<50
50- 100
>100
Surface area (µm²)

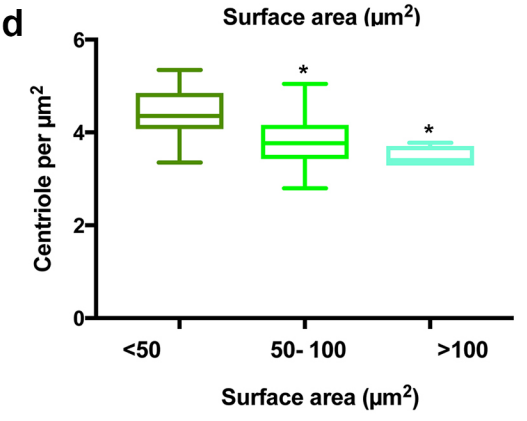
d
Centriole per µm²
0
2
4
6
*
*
<50
50- 100
>100
Surface area (µm²)

Figure 7

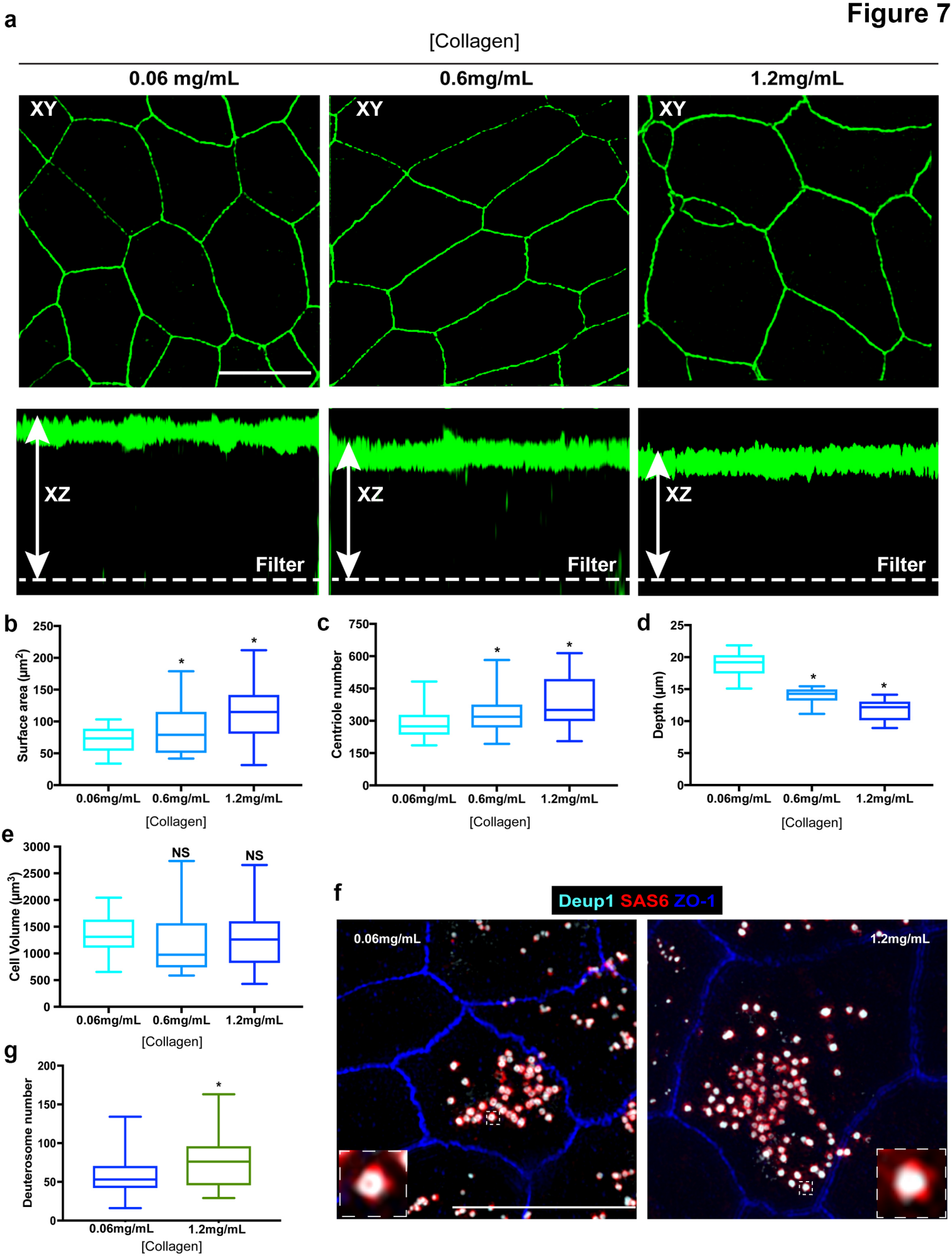
a
[Collagen]
0.06 mg/mL
0.6mg/mL
1.2mg/mL
XY
XZ
Filter
b
Surface area (µm²)
c
Centriole number
d
Depth (µm)
0.06mg/mL
0.6mg/mL
1.2mg/mL
[Collagen]
e
Cell Volume (µm³)
NS
g
Deuterosome number
f
Deup1 SAS6 ZO-1

Supplementary Figure 1

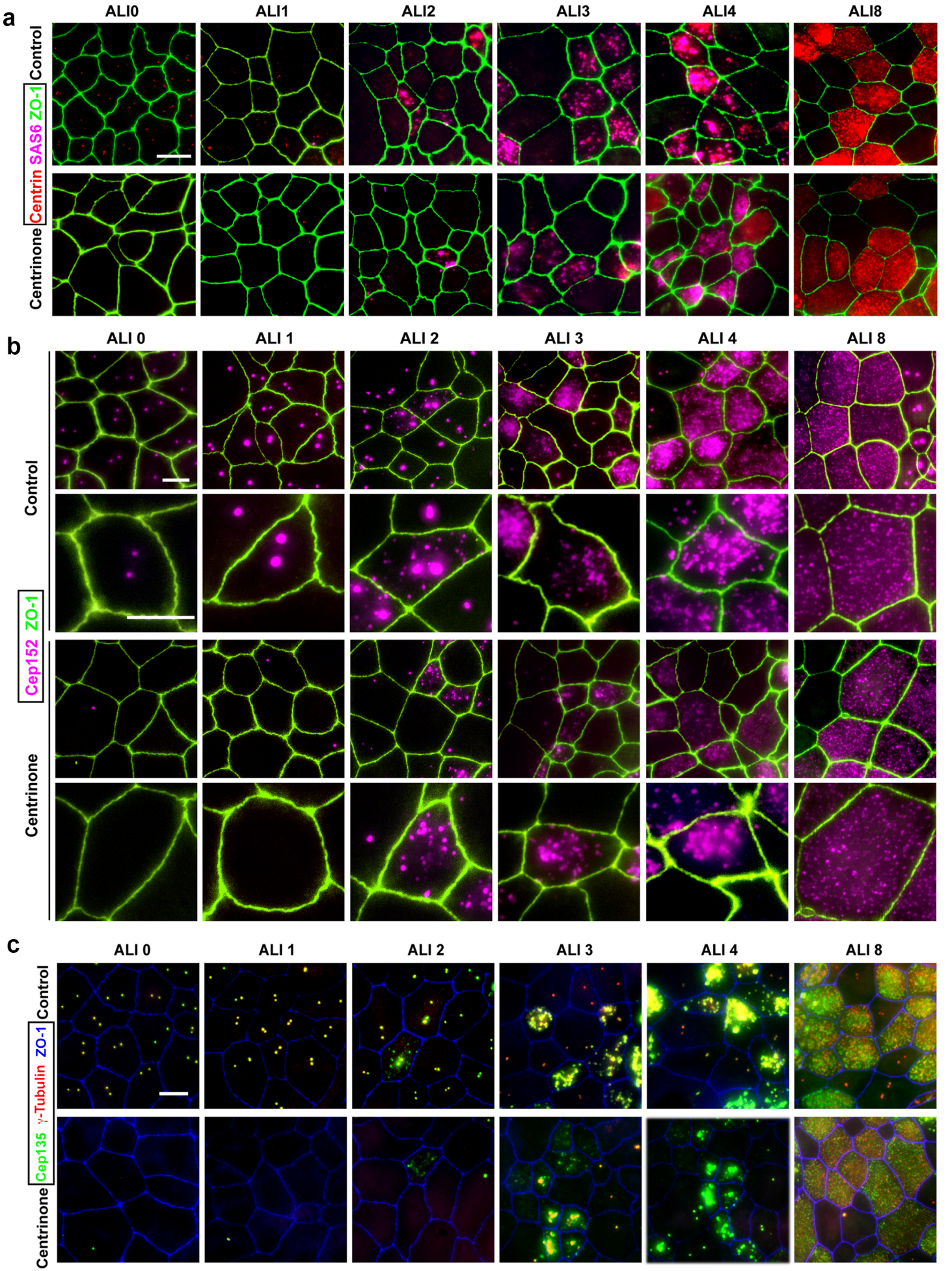

Supplementary Figure 2

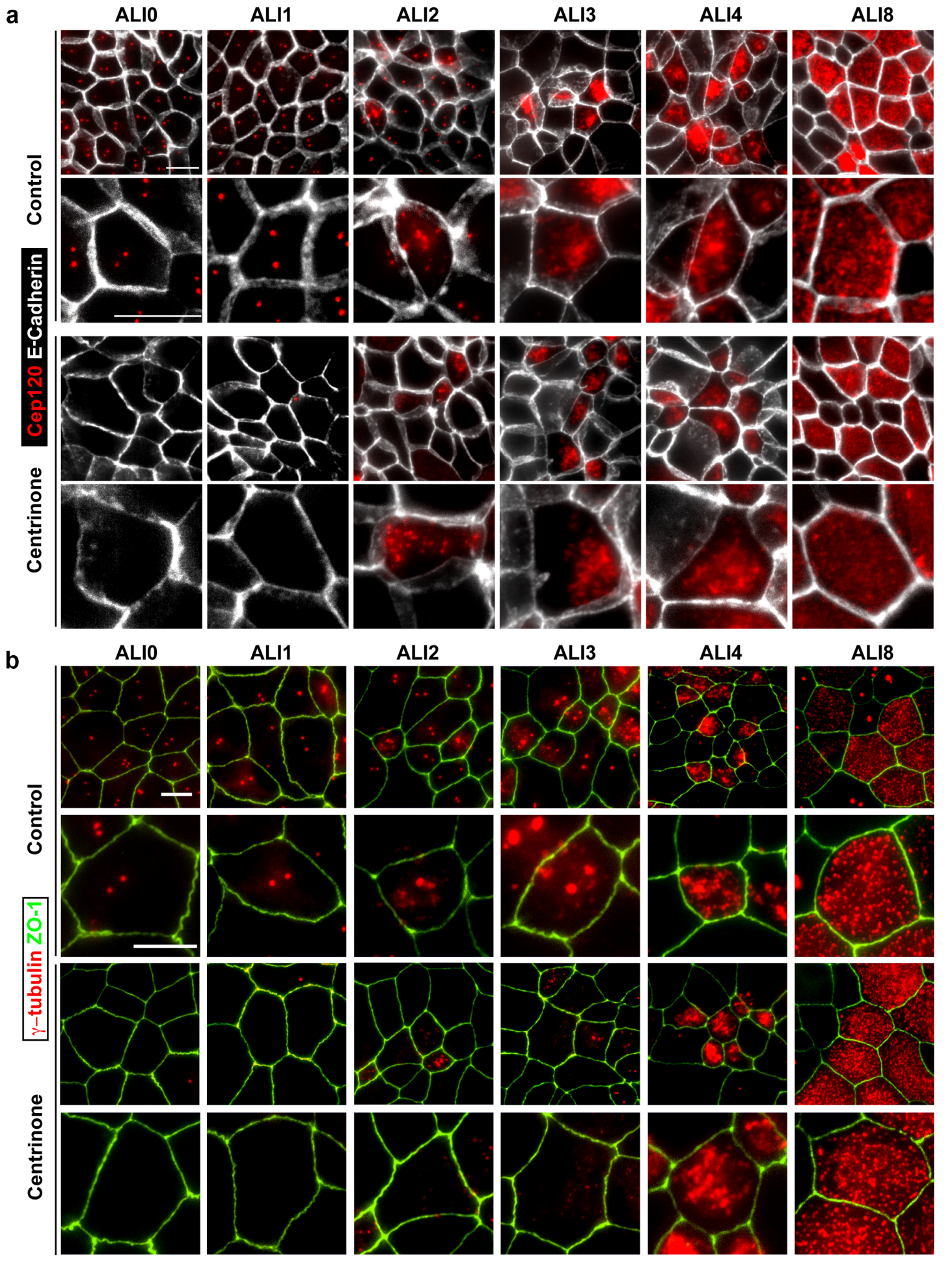

Supplementary Figure 3